Sci Eng Compos Mater 18 (2011): 109–116 © 2011 by Walter de Gruyter • Berlin • Boston. DOI 10.1515/SECM.2011.014

Application of fiber optic sensors for elevated temperature testing of polymer matrix composite materials

John Montesano*, Marina Selezneva, Cheung Poon, Zouheir Fawaz and Kamran Behdinan

Department of Aerospace Engineering, Ryerson University, 350 Victoria St., Toronto, Ontario M5B 2K3, Canada, e-mail: gmontesa@ryerson.ca

*Corresponding author

Abstract

Advanced polymer matrix composite (PMC) materials have been more frequently employed for aerospace applications due to their light weight and high strength. Fiber-reinforced PMC materials are also being considered as potential candidates for elevated temperature applications such as supersonic vehicle airframes and propulsion system components. A new generation of high glass-transition temperature polymers has enabled this development to materialize. Clearly, there is a requirement to better understand the mechanical behaviour of this class of composite materials. In this study, polyimide-coated fiber optic sensors are employed to continuously monitor strain in a woven carbon fiber bismaleimide (BMI) matrix laminate subjected to tensile static and fatigue loading at elevated temperatures. A unique experimental test protocol is utilized to investigate the capability of the optical sensors to monitor strain and track stiffness degradation of the composite material. An advanced interrogation system and an optical spectrum analyzer are utilized to track the variation in the optical fiber wavelength and the wavelength spectrum for correlation with strain gage measurements. Isothermal tensile static and fatigue tests at room temperature, 105°C, 160°C and 205°C suggest that these optical sensors are capable of continuously monitoring strain and tracking the stiffness loss of a highly compliant PMC specimen during cyclic loading. The results illustrate that employing optical sensors for elevated temperature applications has significant advantages when compared to conventional strain gages.

Keywords: elevated temperatures, fatigue testing, fiber bragg grating (FBG), polymer matrix composites (PMC), strain monitoring.

1. Introduction

In recent years, advanced PMC materials have been more frequently employed for aerospace applications due to their high strength-to-weight and stiffness-to-weight ratios. This is exemplified by considering modern commercial transport aircraft such as the Airbus A380 and the Boeing 787. PMC materials are also gaining substantial consideration for elevated temperature applications, such as supersonic vehicle airframes and jet engine components. These materials may be adequate replacements for their metallic counterparts for manufacturing aircraft components exposed to long-term temperatures in the 150–350°C range. A new generation of high glass-transition temperature (T_g) polymers has enabled this development to be achieved. Commercially available polymers such as PMR-15 [1] and bismaleimide (BMI) [2] polyimide resins have been used or are being considered as matrix constituents in fiber-reinforced composite materials to manufacture jet engine components or supersonic vehicle airframe components. Clearly, there is a requirement to better understand the mechanical behavior of this class of PMCs to ensure their widespread use for these applications.

As a result, a number of experimental programs based on elevated temperature mechanical testing of this class of PMCs have been developed and conducted in recent years. The complexity in devising an appropriate experimental protocol and employing an adequate testing apparatus is increased due to the elevated testing temperatures, which poses great difficulties for researchers. Both tensile static tests [3–5] and fatigue tests [6–9] have been conducted at elevated temperatures for various PMC materials. These studies employ various heating sources and either cooled hydraulic grips or mechanical gripping fixtures for load application. In addition, these studies utilize either strain gages or extensometers to monitor the strain (or stiffness) during mechanical testing. Note that during cyclic loading, strain gage and extensometer capabilities may be significantly limited. Strain gages have a much lower strain limit during cyclic loading when compared to their static strain limit [10], while extensometers become unreliable at higher strains and loading frequencies, due to slipping of the probe edges with the specimen surface [11]. A remedy is to interrupt the fatigue test at specific intervals and conduct a static test with extensometers in place [12], as is specified in testing standard ASTM D 3479 [13]. This is seen as a limitation since it does not allow for continuous strain measurement during cycling, which may be required for properly tracking stiffness degradation throughout the entire life of the specimen [14–16]. This is also a serious limitation for determining fatigue lives of materials that exhibit load-time dependency since the time during which the test is paused and/or loaded monotonically can affect the materials fatigue response.

Fiber Bragg grating (FBG) sensors have been employed in many studies for both strain and damage monitoring of PMCs, and are considered ideal candidates for high-strain

magnitude fatigue loading of PMCs at elevated temperatures. FBG sensors may provide a solution to overcome the limitations of more conventional dynamic strain monitoring techniques such as strain gages and extensometers. Embedding and surface mounting FBG sensors have been shown to have minimal impact on the bulk properties of PMC materials due to their small diameter [17]. Another advantage of employing FBG sensors for elevated temperature fatigue testing is that the effects of strain and temperature on the sensor can in fact be isolated [18, 19]. Many studies [20–26] have successfully demonstrated the ability of embedded FBG sensors to measure internal strains and temperature, and to detect damage such as matrix cracking and ply delamination in PMC laminates. All studies clearly state that there are limitations with embedding optical fibers, specifically the complexity of manufacturing a composite with embedded optical sensors. In order to alleviate some of the complications of embedding FBG sensors, the sensors can be mounted on the surface of a specimen or component. DeBaere et al. [17] revealed that both embedded and surface mounted FBGs perform well for strain monitoring in a thermoplastic matrix laminate subjected to cyclic loading. There are few studies that employ FBG sensors for strain or stiffness monitoring during fatigue loading of composite materials, mainly due to the difficulty in the interrogation of the cyclic waveform data. Also to the knowledge of the authors, FBG sensors have not been utilized for elevated temperature fatigue testing of any PMC materials.

In this study, high temperature polyimide-coated FBG sensors are assessed for their ability to continuously measure strain in a woven PMC laminate subjected to tensile static and fatigue loading at various temperatures up to 205°C. The subsequent section includes a brief review of the theory and concepts of FBG sensors applicable to this study, which is followed by an overview of the experimental set-up and the experimental test program. The experimental test results are then presented and discussed, and a final conclusion section outlines the significant findings of this study as well as recommendations for future work.

2. Fiber Bragg grating theory

The basic principle for a uniform optical FBG sensor located in a single mode coated optical fiber is illustrated schematically in Figure 1. The gratings used in this study have a constant pitch (Λ) and length (L), and an index of refraction denoted by n. Figure 2 shows a schematic of the wavelength spectrum of a broadband light source into a uniform FBG sensor, with the Bragg wavelength denoted by λ_B. Further details about FBG sensor operation and manufacturing can be found in the literature [20, 27].

The Bragg wavelength for the reflected spectrum of the grating is defined by:

$$\lambda_B = 2n\Lambda \tag{1}$$

Any change in either n or Λ will cause the Bragg wavelength to shift, which will facilitate determination of the strain and temperature environment to which the optical fiber is subjected in this study. The shift in the Bragg wavelength due to both strain and temperature is obtained by [27]:

$$\Delta\lambda_B = 2n\Lambda\left(\left\{1-\left(\frac{n^2}{2}\right)\left[P_{12}-\nu\left(P_{11}+P_{12}\right)\right]\right\}\varepsilon + \left[\alpha+\frac{dn/dT}{n}\right]\Delta T\right) \tag{2}$$

The applied strain and temperature change are, respectively, denoted by ε and ΔT, P_{11} and P_{12} are Pockel's coefficients of the stress-optic tensor and ν and α are the Poisson's ratio and coefficient of thermal expansion of the fiber material, respectively. Using the material parameters for the silica glass fibers used in this study, the factor $\left\{1-\left(n^2/2\right)\left[P_{12}-\nu\left(P_{11}+P_{12}\right)\right]\right\}$ has a definite value of 0.7981. Thus, the strain response at a constant temperature is found to be:

$$\frac{\Delta\lambda_B}{2n\Lambda} = (0.7981)\varepsilon \tag{3}$$

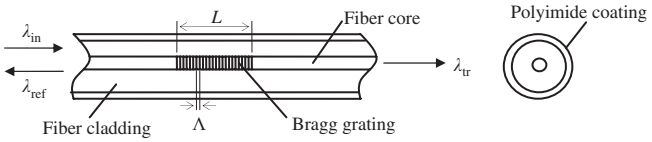

Figure 1 The principle of a conventional uniform FBG sensor.

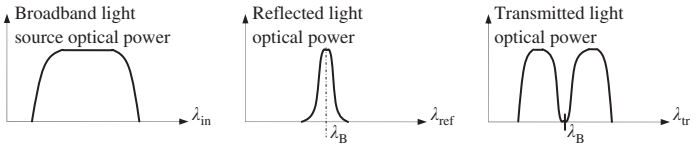

Figure 2 Schematic of light wavelength spectrum through a FBG sensor.

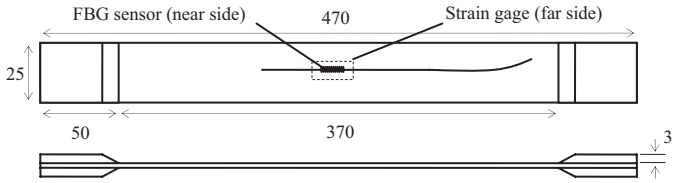

Figure 3 Test specimen geometry (all dimensions in mm).

In this study, the temperature is constant during mechanical loading, thus Eq. (3) is used for the strain calculations based on the measured shift in the Bragg wavelength.

3. Materials and methods

3.1. Materials

The material used for the experiments was a two-dimensional woven T650-35 3K carbon fiber-reinforced 5250-4 BMI resin. The fibers and matrix are both commercially available constituents. The laminate panel consisted of six plies of the woven carbon/BMI, with the weave direction of all plies at 45° bias from the loading axis. The panel was supplied by a third party and, as such, any manufacturing information is unavailable for disclosure. The final panel had dimensions of 470×190 mm. The test specimens for static and fatigue tests were cut to nominal dimensions of 470×25 mm using an abrasive waterjet cutting technique. Tapered aluminum end tabs 50 mm in length were then bonded to each specimen as shown in Figure 3. The angle of taper for each end tab was 25°. The specimen geometry is in compliance with that specified in testing standard ASTM D 3479 [13]. A specimen length of 470 mm was used in order to allow the end tabs to sufficiently protrude outside of the heating furnace for gripping (see Figure 5).

Strain gages and FBG sensors were subsequently bonded to each test specimen. Vishay EA series resistance strain gages were used for the room temperature (RT) tests, while Vishay WK series resistance strain gages were employed for the elevated temperature tests. The FBG sensors were all written in single mode glass optical fibers, with grating lengths ranging from 5 mm to 8 mm. In addition, the optical fibers used for the elevated temperature tests were coated with a polyimide coating, yielding a total diameter of 160 µm. For the RT tests, Loctite 496 RT curable adhesive was used to bond both the strain gage and the FBG sensors, while for the elevated temperature tests M-Bond 610 adhesive was used. The strain gage and FBG sensor for each specimen were bonded at the center of the test specimen on opposing sides as shown in Figure 3. This was done to allow for a direct comparison between the strain gage and FBG. In each case, the local specimen surface was prepared for bonding (i.e., degreaser, abrasion, conditioner and neutralizer). For the FBG sensor, the grating was positioned on the specimen and pre-strained by using high temperature Kapton tape on either end of the grating. The pre-strain on the fiber caused a slight shift in the Bragg wavelength, which resulted in a strain of ~100 microstrains. This was done to prevent buckling of the fiber during unloading of the tensile test specimens. Next, the fiber was bonded over the entire length of the grating using the corresponding adhesive. For the elevated temperature test specimens where M-Bond 610 adhesive was used, additional pressure was applied to the fiber for curing. The adhesive was cured in air at 165°C for 1.5 h. A photograph of the externally bonded FBG sensor is shown in Figure 4.

3.2. Experimental setup

All static and fatigue tests were performed using an MTS 322 loading frame with an MTS FlexTest GT/Teststar IIm controller and data acquisition unit. A linear servo-hydraulic actuator provided the load input, where a 250 kN load cell and a linear variable displacement transducer (LVDT) provided load and displacement feedback for the controller, respectively. Hydraulic wedge grips, which remained out of the furnace heat zone during the elevated temperature tests, were used to grip the specimens. Multi-channel data for the load cell, LVDT and strain gage were acquired with MTS software through a PC connected to the data acquisition unit. The strain gage terminals were connected to a P3 strain indicator unit, which provided an analog signal (i.e., voltage) as input for the MTS FlexTest GT/Teststar IIm. This ensured that the acquired load cell, LVDT and strain gage data were properly time-stamped and synchronized. It should be noted that extensometers were not used in this study due to encountered difficulties of contact between the extensometer blades and the test specimens during fatigue loading.

An ATS 3210 electric clam-shell type furnace with an integrated temperature controller was used as a heat source for the test specimen gage section for all elevated temperature tests. The furnace included three heating zones, each consisting of a K-type thermocouple for temperature feedback to the controller. The length of the furnace was 240 mm, with a 50 mm diameter test section. The temperature controller PID parameters and power output values were adjusted as to provide a gradual rise in the furnace temperature of 0.2°C/s during

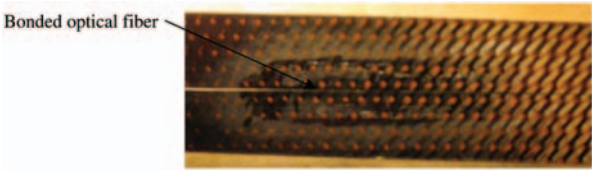

Figure 4 Photograph of surface bonded FBG sensor.

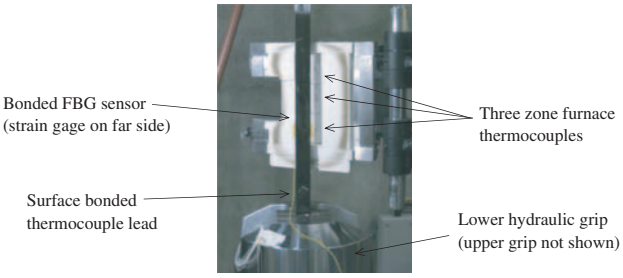

Figure 5 Photograph of gripped test specimen in opened furnace.

temperature ramp-up to the final test temperature. Once the test temperature was reached, the specimen was allowed to stand for 20 min to ensure uniform temperature in the gage section. The settings on the temperature controller ensured a uniform test temperature in the furnace and a constant test temperature throughout the duration of all tests within ±2°C, which is in accordance with ASTM D 3479 test standard [13]. An additional K-type thermocouple was bonded to the surface of the specimen using high temperature Kapton tape to monitor the surface temperature during fatigue testing. A photograph of a gripped test specimen in the opened furnace is included in Figure 5.

A Micron Optics si425 optical sensing interrogator with integrated light source was employed to continuously capture the dynamic reflected FBG wavelength peaks during both static and fatigue loading. The interrogator has a maximum sampling frequency of 250 Hz, and can simultaneously capture 4 channels of data from 4 optical fibers with up to 100 FBG sensors per fiber. The range of Bragg wavelengths for all FBG sensors used in this study are in the C-band region (1520–1570 nm), which is the sensing range of the optical sensing interrogator. The interrogator has the single option of saving time-stamped peak wavelength data for the FBG sensors. In this study, there was no attempt to synchronize the interrogator data with the MTS data acquisition unit. Post-processing algorithms were employed to synchronize the time-scale data of the peak wavelength values and the load, displacement and strain values. It was also necessary for this study to capture the entire reflected spectrum for static tests conducted at predefined intervals during fatigue testing. To achieve this, an Ando Aq6331 optical spectrum analyzer (OSA) with a JDS Uniphase Broadband Light Source and an optical coupler were utilized. The OSA has the ability to save the captured spectrum optical power/wavelength data. Note that due to the low scanning frequency of the OSA, the reflected spectrum can only be scanned during load/displacement dwells for static tests. Schematics of the experimental setup with both the si425 interrogator and the OSA are shown in Figure 6.

3.3. Experimental test program

A number of static tensile tests were initially conducted at RT and elevated temperatures to monitor the time-dependent behavior of the material and the corresponding response of the FBG sensors. These tests provided a suitable correlation for FBG sensor and strain gage measurements. In total, two types of static tests were conducted under displacement control. The first test consisted of a ramp-up to a displacement of 2.5 mm with the subsequent ramp-down to near-zero displacement, both at a rate of 0.6 mm/min. The second test consisted of a series of ramp-up and dwells for three displacement values (1.0 mm, 2.0 mm, 2.5 mm), at a rate of 0.2 mm/s. In this study specimens were tested at RT, 105°C and 205°C.

The subsequent set of tests were isothermal uniaxial tension-tension fatigue tests conducted at RT, 105°C, 160°C and 205°C under load control with a constant amplitude sinusoidal waveform. The stress ratio (i.e., minimum stress/maximum stress) was set to 0.1, and the loading frequency was 5 Hz for all tests. All fatigue tests were interrupted at predefined intervals to perform static tests in order to monitor the specimen stiffness using both the interrogator and the OSA. These static tests were conducted in displacement control up to the maximum cyclic stress in accordance with ASTM D 3479 [13]. Although in this study fatigue tests were interrupted at predefined intervals to perform static tests, the long-term goal is to continuously monitor strain using FBG sensors and track the stiffness degradation of a test specimen without interrupting the fatigue test. This methodology will facilitate tracking the stiffness degradation of a test specimen via strain measurements during a load controlled fatigue test.

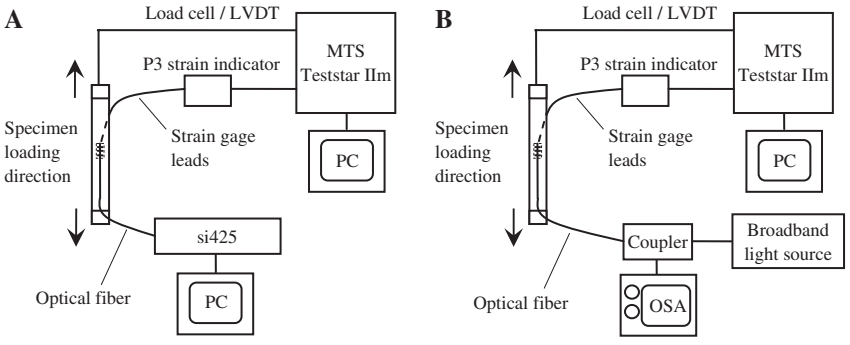

Figure 6 Schematic of experimental setup (A) Interrogator, (B) OSA.

4. Results and discussion

4.1. Static tests

The first set of static tests was conducted at RT on the same test specimen as described in the previous section. Figure 7 is a plot of the axial strain versus time as measured by both the FBG sensor and the strain gage for the static test with three dwells. The correlation between the FBG sensor and the strain gage is excellent as shown. The results of the second RT static test with a constant loading/unloading rate are shown in Figure 8. Once again the correlation between the FBG sensor and the strain gage is excellent. The plots in Figures 7 and 8 demonstrate the consistent response of the FBG sensor at two considerably different loading rates. This is a critical requirement for PMC materials that exhibit time-dependent stress-strain behavior since changes in the loading rate result in significantly different material response, which is indeed detected by the FBG sensor. This also illustrates that there is minimal strain transmission loss from the specimen through the adhesive to the FBG sensor, which can frequently occur with surface bonded FBG sensors [26]. Also, the consistency in the wavelength-calculated strain during the displacement dwells is clearly illustrated in the plot. This ensures that the adhesive sufficiently bonds the FBG sensor to the specimen surface.

The second set of static tests was conducted at 105°C on a second test specimen. Figure 9 is a plot of axial strain versus time (similar to Figure 7). Once again, an excellent correlation between the FBG sensor and the strain gage data exists. Note that there is a slight discrepancy between the two strain sensors at the lowest and highest dwells, which may be a result of the slight temperature fluctuations (±2°C) in the specimen gage section. These fluctuations can cause a slight increase or decrease in the measured wavelength value due to the sensitivity of the FBG sensor to the change in temperature. Although this slight discrepancy does exist, the differences in the magnitude of the calculated strain values do not deviate by more than 5% when compared to the strain gage values.

4.2. Fatigue tests

The tension-tension fatigue tests were all conducted until specimen failure occurred. Due to the high strain levels of each test, the elevated temperature specimens tested at 105°C, 160°C and 205°C failed prior to 100,000 load cycles. The RT specimen endured for approximately 280,000 load cycles. For all conducted fatigue tests the FBG sensor remained bonded

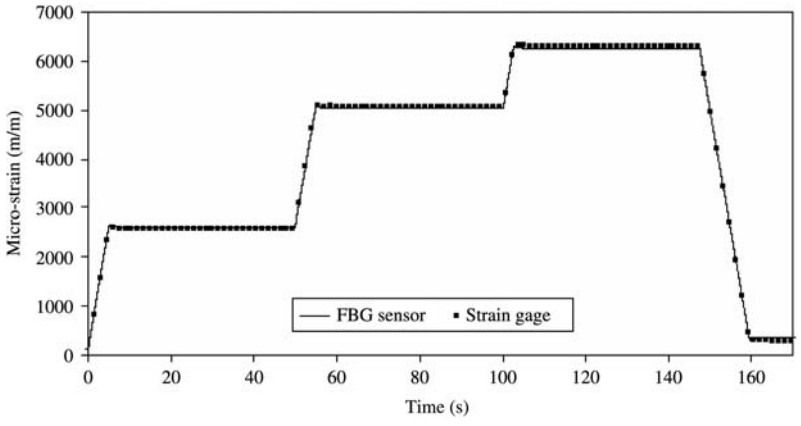

Figure 7 RT static tensile test with dwells.

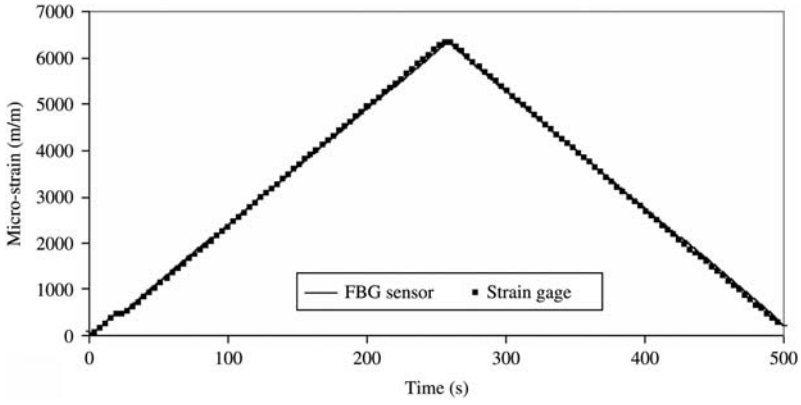

Figure 8 RT static tensile test.

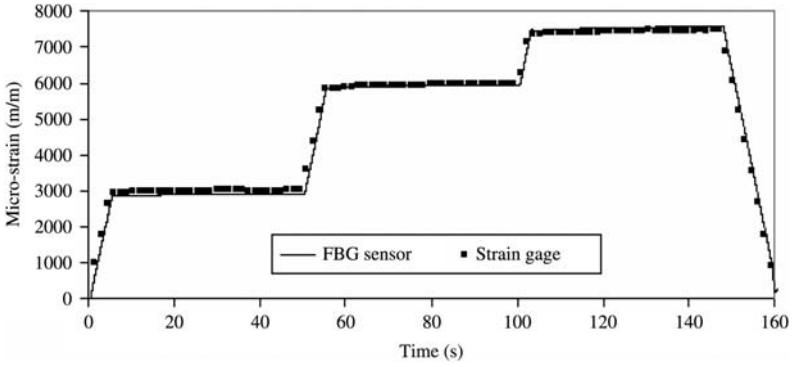

Figure 9 Elevated temperature static tensile test with dwells.

and undamaged for the duration of the test, while the strain gages failed well before specimen failure. This illustrates that at elevated temperatures and high cyclic strain levels FBG sensors are indeed reliable, while high temperature strain gages are not suitable.

In order to illustrate the FBG sensor accuracy for dynamic strain measurement, the strain was calculated from the measured change in central wavelength using Eq. (3). These values were then correlated to the measured strains from the resistance strain gage for all fatigue tests. Recall that the strain gages were bonded on the specimen surface directly opposite from the FBG sensor (see Figure 3). A plot of axial strain versus load cycles for the RT fatigue test is shown in Figure 10. The correlation between the strain gage and the FBG sensor is excellent, with <1% deviation in the strain data. Similar correlations were drawn for all elevated temperature fatigue tests. A similar plot for the 205°C fatigue test is shown in Figure 11. Once again, there is an excellent correlation between the strain gage and the FBG sensor. Note that similar correlations could not be made later in the fatigue tests at higher loading

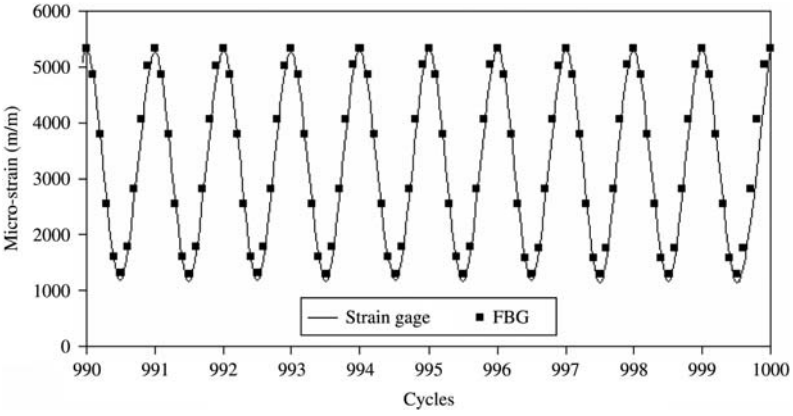

Figure 10 Strain versus load cycles: RT fatigue test.

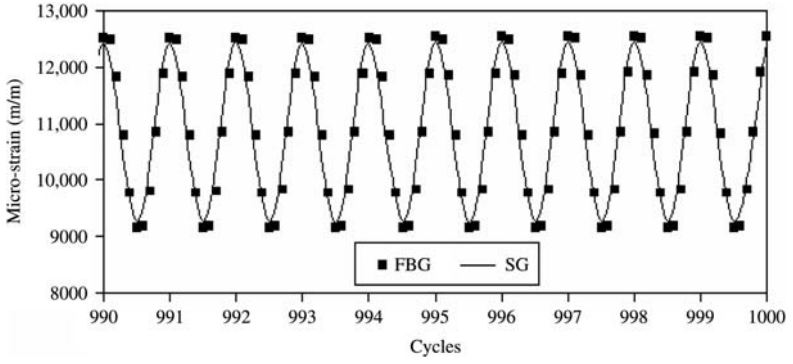

Figure 11 Strain versus load cycles: 205°C fatigue test.

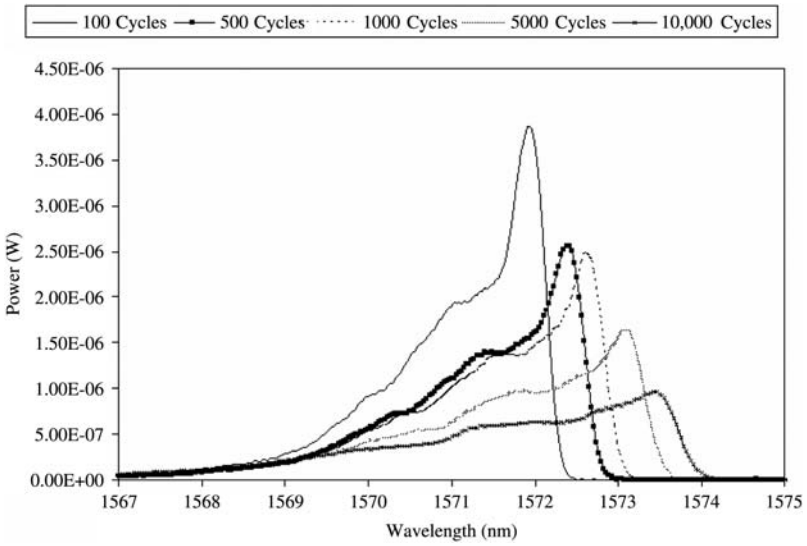

Figure 12 Wavelength spectra for 205°C fatigue test.

cycles, due to premature failure of the strain gage. Also, note that for the elevated temperature tests it was found that the surface temperature of the specimens increased slightly during cycling due to self-generated heating. The slight deviations in Figure 11 can be attributed to this effect.

In addition to monitoring the strain, the ability of the FBG sensors to track the specimen permanent deformation was investigated. As indicated, the fatigue tests were interrupted at specific intervals in order to conduct static tests to utilize the capability of the OSA to capture the entire wavelength spectrum. Tracking the change in the spectrum at cyclic intervals facilitates the monitoring of the specimen permanent deformation. Figure 12 is a plot of the successive wavelength spectra for the 205°C test. The plot includes captured spectra after cyclic loading of the specimen for 100, 500, 1000, 5000 and 10,000 cycles. The decrease in the intensity of the peak wavelength and the corresponding increase in the wavelength magnitude are apparent as the loading cycle number increases. This is evidence of increasing strain during the fatigue test since the wavelength increases under the same stress level. Permanent deformation may be due to a combination of local damage and time-dependent creep response of the matrix at the elevated temperature. Similar trends were observed for the 105°C and 160°C fatigue tests, and to a lesser extent for the RT fatigue test. This material behavior is not the focus of this study and as such, is not quantified in this paper; however, the ability of the FBG sensors to track this type of behavior has been proven.

The changes in the corresponding specimen stiffness and permanent deformation can also be illustrated through the successive load-wavelength curves for each individual fatigue test (these are analogous to stress-strain curves). Figure 13 shows a series of plots of applied load versus the FBG sensor wavelength for the 205°C fatigued specimen at the indicated cyclic intervals. The permanent deformation of the specimen is clearly increasing as the number of cycles increases, while the

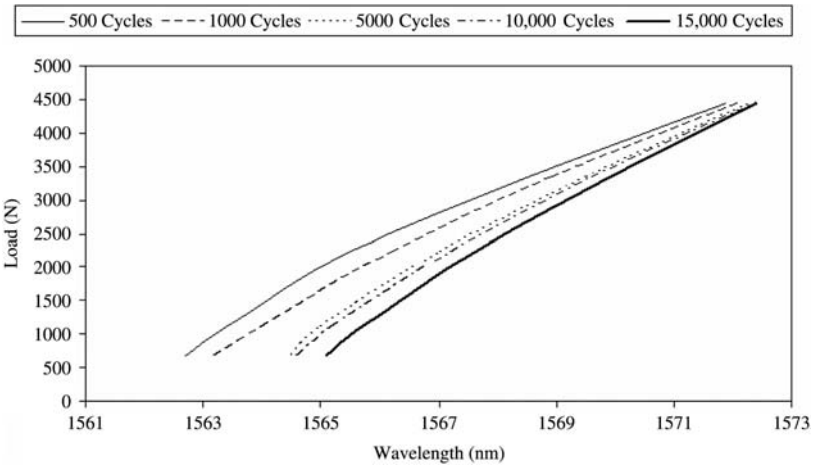

Figure 13 Successive stress versus strain curves for 205°C fatigue test.

change in stiffness can also be seen by observing the successive curves. Once again, to emphasize, the stiffness change of the specimen is not quantified in this paper, whereas the ability of the FBG sensors to track this behavior has been shown.

5. Conclusion

To facilitate continuous strain monitoring for a PMC laminate during elevated temperature tensile static and fatigue testing, polyimide coated FBG sensors were employed. A unique experimental protocol consisting of an advanced interrogation system and an OSA unit were necessary for tracking the measured wavelength data of the optical fibers. Static test results demonstrate that FBG sensors can accurately monitor the strain and are capable of monitoring the time-dependent behavior of the PMC material. Fatigue test results at both room temperature and elevated temperatures confirm that externally bonded FBG sensors accurately measure dynamic axial strain when compared to a conventional resistance strain gage. Minimal strain transmission loss was exhibited by the FBG sensor, with only minor deviations at elevated temperatures due to the slight temperature fluctuations of the furnace or self-generated heating of the specimen during cyclic loading. This deviation can be mitigated by adding a second FBG sensor on the optical fiber which is not bonded to the specimen surface [21]. This second sensor would effectively act as a "thermocouple", providing the shift in wavelength due solely to temperature change and thus providing the correction for the strain induced wavelength shift of the first FBG sensor. In addition, the FBG sensors were capable of operating sufficiently for the duration of each high-strain cyclic test (i.e., until specimen failure), which is seen as an advantage over conventional resistance strain gages and extensometers. As indicated, the strain gages did not withstand the high-strain dynamic loading at elevated temperatures, failing long before the fatigue tests terminated. The capability of the FBG sensors to monitor permanent deformation and stiffness degradation during cyclic loading was also shown.

Additional work may be required to ensure the usefulness of FBG sensors for elevated temperature cyclic testing of other highly compliant PMC materials; however, their ability to continuously measure strain and track stiffness degradation is promising at this stage and is a novel contribution. Additional testing will be conducted on various types of polymer matrix composites at various elevated temperatures to further validate the current results. Also, various high temperature adhesives will be tested for bonding the FBG sensors to ensure repeatability of the presented results.

Acknowledgements

The authors would like to gratefully acknowledge the financial support of the Natural Sciences and Engineering Research Council (NSERC) of Canada (CRD program) and the Consortium for Research and Innovation in Aerospace in Quebec (CRIAQ). The authors would also like to thank Dr. X. Gu of the Department of Electrical Engineering at Ryerson University for supplying the FBG sensors. Finally, the first two authors greatly acknowledge additional funding in the form of scholarships by NSERC.

References

[1] Vannucci RD. *Proceedings of the 32nd International SAMPE Symposium and Exhibition*, Anaheim, 1987.
[2] Shimokawa T, Kakuta Y, Hamaguchi Y, Aiyama T. *J. Composite Mater.* 2008, 42, 655–679.
[3] Wang JZ, Parvatareddy H, Chang T, Iyengar N, Dillard DA, Reifsnider KL. *Composites Sci. Tech.* 1995, 54, 405–415.
[4] Odegard G, Kumosa M. *Composites Sci. Tech.* 2000, 60, 2979–2988.
[5] Cao S, Wu Z, Wang X. *J. Composite Mater.* 2009, 43, 315–330.
[6] Kawai M, Yajima S, Hachinohe A, Kawase Y. *Composites Sci. Tech.* 2001, 61, 1285–1302.
[7] Kawai M, Maki N. *Int. J. Fatigue* 2006, 28, 1297–1306.
[8] Shimokawa T, Kakuta Y, Saeki D, Kogo Y. *J. Composite Mater.* 2007, 41, 2245–2265.
[9] Jen MHR, Tseng YC, Kung HK, Huang JC. *Compos. Part B* 2008, 39, 1142–1146.
[10] Case SW, Plunkett RB, Reifsnider KL, In *High Temperature and Environmental Effects on Polymeric Composites Vol. 2 (ASTM STP 1302)*, Gates TS, Zureick AH, Eds., Philadelphia, 1997, 35–49.
[11] Gyekenyesi AL, Castelli MG, Ellis JR, Burke CS. *NASA Technical Report, TM-106927*, 1995.
[12] Branco CM, Eichler K, Ferreira JM. *Theo. App. Fract. Mech.* 1994, 20, 75–84.
[13] ASTM D 3479/D 3479M -96, *ASTM International,* 2007.
[14] Hwang W, Han KS. *J. Composite Mater.* 1986, 20, 154–165.
[15] Jen MHR, Kau YS, Wu IC. *Int. J. Fatigue* 1994, 16, 193–201.
[16] Whitworth HA. *Compos. Struct.* 1998, 40, 95–101.
[17] DeBaere I, Luyckx G, Voet E, VanPaepegem W, Degrieck J. *Opt. Lasers Eng.* 2009, 47, 403–411.
[18] Tanaka N, Okabe Y, Takeda N. *Smart Mater. Struct.* 2003, 12, 940–946.
[19] Yang B, Tao X, Yu J. *J. Industrial Textiles* 2004, 34, 97–115.
[20] Tao X, Tang L, Du W, Choy C. *Compos. Sci. Tech.* 2000, 60, 657–669.
[21] Montanini R, D'Acquisto LD. *Smart Mater. Struct.* 2007, 16, 1727–1735.
[22] Takeda N. *Int. J. Fatigue* 2002, 24, 281–289.
[23] Takeda S, Okabe Y, Takeda N. *Compos. Part A* 2002, 33, 971–980.
[24] Okabe Y, Tsuji R, Takeda N. *Compos. Part A* 2004, 35, 59–65.
[25] Botsis J, Humbert L, Colpo F, Giaccari P. *Opt. Lasers Eng.* 2005, 43, 491–510.
[26] Li WY, Cheng CC, Lo YL. *Sensor Actuat. A: Phys*. 2009, 149, 201–207.
[27] Kersey AD, Davis MA, Patrick HJ, LeBlanc M, Koo KP, Askins CG, Putnam MA, Friebele EJ. *J. Lightwave Tech.* 1997, 15, 1442–1463.